NONLINEAR STAGE OF HOSE INSTABILITY

Yu. A. Berezin

We examine the one-dimensional problem of hose instability development in an anisotropic plasma and its effect on the shock wave structure. It is shown that for comparatively small times after instability initiation the magnetic field performs regular oscillations which become stochastic for large times and the system transitions to the turbulent regime. The one-dimensional model of an anisotropic plasma is unstable with respect to growth of Alfven waves under the conditions

$$p_\parallel > p_\perp + \frac{H_0^2}{4\pi}, \quad kR < 2\left[\frac{1}{p_\parallel}\left(p_\parallel - p_\perp - \frac{H_0^2}{4\pi}\right)\right]^{1/2}, \quad R = \frac{1}{\omega}\left(\frac{p_\parallel}{\rho}\right)^{1/2}$$

where $p_\parallel$ ($p_\perp$) is the plasma pressure along (across) the unperturbed magnetic field H_0, R is the ion Larmor radius, k is the perturbation harmonic wavenumber.

1. Exact Solution in a Particular Case. If the initial perturbation is a monochromatic wave with circular polarization then, as shown in [1], the problem of the nonlinear stage of hose instability admits an analytic solution of the form

$$H_x = H_0 B(t) \sin(kz + \varphi(t)), \quad H_y = H_0 B(t) \cos(kz + \varphi(t)) \tag{1.1}$$

where the amplitude B(t) and phase $\varphi(t)$ satisfy the equations

$$\varphi' = -\frac{\omega_0}{B^2}\left[1 + \frac{4}{3}\alpha + \frac{2}{3}\alpha(B^2 - 2)\sqrt{1+B^2} - \frac{1}{1+B^2}\right] \tag{1.2}$$

$$\omega_0 = {}^1/_2\omega k^2 R^2, \qquad \alpha = p_\perp^\circ / p_\parallel^\circ$$

$$B'^2 + U(B) = E = \text{const} \tag{1.3}$$

The potential energy is

$$U(B) = \frac{k^2 p_\parallel^\circ}{\rho_0}\left(\frac{1}{1+B^2} + 2\alpha\sqrt{1+B^2} + \frac{H_0^2}{4\pi p_\parallel^\circ}B^2\right) + \omega_0^2\left[\frac{\alpha^2}{9}\left(\frac{32}{B^2} - 12B^2 + 4B^4 - \frac{32\sqrt{1+B^2}}{B^2} + 16\sqrt{1+B^2}\right)\right.$$
$$\left. + \frac{4}{3}\alpha\left(\sqrt{1+B^2} - \frac{2B^2}{1+B^2} - \frac{3}{\sqrt{1+B^2}}\right) + \frac{1+2B^2}{1+B^2} - \frac{B^4}{(1+B^2)^2}\right] \tag{1.4}$$

The total energy E is defined by the magnitude of the initial perturbation and equals

$$E = \gamma^2 B'^{(\circ)2} + U(B^{(\circ)})$$
$$\gamma = \omega k R\left[\frac{1}{p_\parallel^\circ}\left(p_\parallel^\circ - p_\perp^\circ - \frac{H_0^2}{4\pi}\right) - \frac{1}{4}k^2R^2\right]^{1/2} \tag{1.5}$$

Here γ is the small-perturbation growth increment, obtained from linear theory. In the limiting case of quite small but finite perturbations the amplitude of the nonlinear monochromatic wave with circular polarization is proportional to the hose instability increment

$$B_{\max} = \frac{\gamma}{\omega k R\sqrt{1 - {}^1/_4\alpha - {}^1/_2(1 - {}^1/_2\alpha)k^2R^2}} \tag{1.6}$$

Hence this limiting case will hold for sufficiently small increments γ. Substituting the expression for the increment into (1.6), we obtain

Novosibirsk. Translated from Zhurnal Prikladnoi Mekhaniki i Tekhnicheskoi Fiziki, Vol. 11, No. 3, pp. 3-10, May-June, 1970. Original article submitted May 14, 1969.

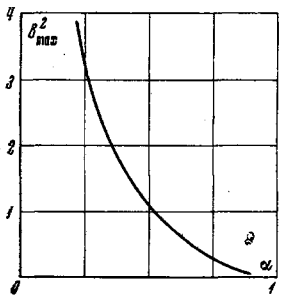

Fig. 1

$$B_{\max} = \left[\frac{1 - \alpha - H_0^2/(4\pi p_\parallel^\circ) - 1/4 k^2R^2}{1 - 1/4\alpha - 1/2(1 - 1/2\alpha)\, k^2R^2}\right]^{1/2} \tag{1.7}$$

In the case of sufficiently long perturbations ($kR \to 0$) and small anisotropy of the plasma ($p_\perp^\circ \sim p_\parallel^\circ$; $p_\parallel^\circ$, $p_\perp^\circ \gg H_0^2/8\pi$) we have

$$B_{\max} = \left(\frac{4}{3}\frac{\Delta p}{p_\parallel^\circ}\right)^{1/2}, \qquad \Delta p = p_\parallel^\circ - p_\perp^\circ - H_0^2/4\pi \tag{1.8}$$

Thus, for small plasma anisotropy the maximal amplitude of the nonlinear wave is proportional to the square root of the degree of plasma anisotropy.

To determine the maximal wave amplitude in an arbitrary case we solved numerically the transcendental equation $U(B_{max}) = E$, where $U(B)$ is given by (1.4) and E by (1.5). Figure 1 shows the resulting curve of the maximal wave amplitude squared versus the pressure ratio $\alpha = p_\perp^\circ/p_\parallel^\circ$ (the calculation was made for $p_\parallel^\circ = 30H_0^2/8\pi$, $\lambda = 80R$ is the initial perturbation wavelength). For small anisotropy ($\alpha \to 1$) the amplitudes B_{max} are small and agree with the values obtained using (1.7). For large anisotropy (sufficiently small α) B_{max} increases sharply, reaching values $B_{max} \simeq 2$ for $\alpha = 0.2$.

2. Numerical Solution Method. For perturbations of arbitrary type an analytic solution of the problem in the nonlinear hose instability stage cannot be found. Therefore we made a numerical study, some results of which were presented previously in [1].

Basic Equations. The system of equations describing the one-dimensional anisotropic plasma model in dimensionless variables has the form

$$\frac{\partial \rho}{\partial t} + \frac{s}{V_A}\frac{\partial}{\partial z}(\rho w) = 0$$

$$\frac{\partial M}{\partial t} + \frac{V_A}{2s}\frac{\partial}{\partial z}\left(3aMw + p_\perp + \frac{p_\parallel - p_\perp}{1 + H_x^2 + H_y^2} + H_x^2 + H_y^2\right) = 0 \tag{2.1}$$

$$\frac{\partial N}{\partial t} + \frac{\partial}{\partial z}\left\{\frac{s}{V_A}Nw + \left(\frac{1}{2}\frac{p_\parallel - p_\perp}{1 + H_x^2 + H_y^2} - 1\right)H_x - \frac{1}{\sqrt{2a\varkappa}}\left[\frac{s}{V_A}H_y\frac{p_\parallel - p_\perp}{1 + H_x^2 + H_y^2}\frac{\partial w}{\partial z} + \left(p_\perp + \frac{p_\parallel - p_\perp}{1 + H_x^2 + H_y^2}\right)\frac{\partial v}{\partial z}\right]\right\} = 0$$

$$\frac{\partial Q}{\partial t} + \frac{\partial}{\partial z}\left\{\frac{s}{V_A}Qw + \left(\frac{1}{2}\frac{p_\parallel - p_\perp}{1 + H_x^2 + H_y^2} - 1\right)H_y + \frac{1}{\sqrt{2a\varkappa}}\left[\frac{s}{V_A}H_x\frac{p_\parallel - p_\perp}{1 + H_x^2 + H_y^2}\frac{\partial w}{\partial z} + \left(p_\perp + \frac{p_\parallel - p_\perp}{1 + H_x^2 + H_y^2}\right)\frac{\partial u}{\partial z}\right]\right\} = 0$$

$$\frac{\partial H_x}{\partial t} + \frac{\partial}{\partial z}\left(\frac{s}{V_A}H_x w - u\right) = 0 \tag{2.1}$$

$$\frac{\partial H_y}{\partial t} + \frac{\partial}{\partial z}\left(\frac{s}{V_A}H_y w - v\right) = 0$$

$$\frac{\partial}{\partial t}\left(p_\parallel\frac{1 + H_x^2 + H_y^2}{\rho^3}\right) + \frac{s}{V_A}w\frac{\partial}{\partial z}\left(p_\parallel\frac{1 + H_x^2 + H_y^2}{\rho^3}\right) = 0$$

$$\frac{\partial}{\partial t}\frac{p_\perp}{\rho\sqrt{1 + H_x^2 + H_y^2}} + \frac{s}{V_A}w\frac{\partial}{\partial z}\frac{p_\perp}{\rho\sqrt{1 + H_x^2 + H_y^2}} = 0$$

$$V_A = \frac{H_0}{\sqrt{4\pi\rho_0}}, \quad s = \left(\frac{3p_\parallel^\circ}{\rho_0}\right)^{1/2}, \quad R = \frac{1}{\omega}\left(\frac{p_\parallel}{\rho_0}\right)^{1/2}, \quad a = \frac{8\pi p_\parallel^\circ}{H_0^2}, \quad b = \frac{8\pi p_\perp^\circ}{H_0^2}$$

$$L = \varkappa R, \quad M = \rho w, \quad N = \rho u, \quad Q = \rho v$$

The transverse velocities u, v are normed by V_A, the longitudinal velocity by the sound speed s, and distances by the length L of the computational interval ($\varkappa$ is the number of ion Larmor radii R in the computational interval).

Initial and Boundary Conditions. As the initial perturbations for the transverse motion we took the sum of several harmonic circularly polarized waves with different phase shifts, amplitudes, and wave-

lengths. The connection between the amplitudes of the transverse magnetic fields and the transverse velocities was determined from the solution of the linearized system of equations used in linear instability analysis:

$$\begin{aligned} H_x(z,0) &= \sum_{i=1}^{\mu} C_i \cos\left(\frac{2\pi}{\lambda_i} z + f_i\right) \\ H_y(z,0) &= \sum_{i=1}^{\mu} C_i \sin\left(\frac{2\pi}{\lambda_i} z + f1_i\right) \\ u(z,0) &= -\sum_{i=1}^{\mu} C_i \frac{\lambda_i}{2\pi} \cos\left(\frac{2\pi}{\lambda_i} z + \varphi_i + f_i\right) \\ v(z,0) &= -\sum_{i=1}^{\mu} C_i \frac{\lambda_i}{2\pi} \sin\left(\frac{2\pi}{\lambda_i} z + \varphi_i + f1_i\right) \end{aligned} \tag{2.2}$$

Here λ_i is the length of the i-th perturbation harmonic, C_i is the amplitude of this harmonic, and the magnitude of the phase φ_i is found from the equation

$$\varphi_i = \operatorname{arc\,tg}\left[\varkappa\lambda_i\pi^{-1}(1-\alpha-2/a-\pi^2/\varkappa^2\lambda_i^2)^{1/2}\right]$$

If in (2.2) we set $\mu = 1$, $f_i = f1_i = 0$, $C_1 \neq 0$, the initial perturbation will be a circularly polarized monochromatic wave.

To study the influence of hose instability on the shock wave structure we examined the specification of the initial compression pulse in the form of a Riemann wave. If in (2.1) we neglect the transferse motion, for the longitudinal motion we obtain the system of gasdynamic equations with the adiabatic exponent $\chi = 3$, i.e.,

$$\begin{aligned} &\frac{\partial\rho}{\partial t} + \frac{s}{V_A}\frac{\partial}{\partial z}(\rho w) = 0, \quad p = a\rho^3 \\ &\frac{\partial}{\partial t}(\rho w) + \frac{V_A}{2s}\frac{\partial}{\partial s}(3a\rho w^2 + p) = 0 \end{aligned} \tag{2.3}$$

Setting $w = w(\rho)$ and substituting into (2.3), we obtain for the sound wave of finite amplitude, which was selected as the initial perturbation in the longitudinal motion,

$$p(z,0) = a\rho^3(z,0), \qquad w(z,0) = \rho(z,0) - 1 \tag{2.4}$$

In the numerical solution, symmetric initial compression was specified:

$$\rho(z,0) = 1 + A\exp(-z^2/l^2) \tag{2.5}$$

For $A = 0$ we obtain the problem of the development of purely transverse initial perturbations.

As the boundary conditions we took the periodicity conditions for all the unknown functions, i.e.,

$$\Phi(0,t) = \Phi(L,t) \tag{2.6}$$

An explicit difference scheme was used to solve the formulated problem (2.1), (2.2), (2.4)-(2.6).

3. Numerical Solution Results. We noted above that the use in the calculation of the condition (2.5) with $A = 0$ corresponded to the solution of the problem of the evolution of transverse initial perturbations (in the absence of initial longitudinal perturbations).

An extensive series of calculations was made for the case of a single circularly polarized monochromatic wave taken as the initial condition [for this case we must set $\mu = 1$, $f_i = f1_i = 0$, $C \neq 0$ in (2.2)]. For times $t \leq \gamma^{-1}$ the numerical solution coincides with the solution of the linearized system, i.e., all the quantities characterizing the wave grow exponentially with the increment γ. For times $t > \gamma^{-1}$ the nonlinear solution grows more slowly than the linear solution; the magnetic field and the velocity in the wave reach a maximum and then decay. Figure 2 shows the time dependence of the magnetic pressure $p_m = H_\perp^2$ in the Alfven wave obtained from the numerical solution. For comparison the dashed curve shows the time variation of the magnetic field in the linear approximation.

For times $0 < t \leqslant 20\gamma^{-1}$ the magnetic pressure performs regular oscillations whose amplitude and period agree well with the analytic solution. A typical curve of magnetic pressure p_m versus time is pre-

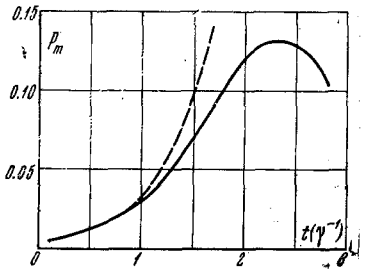

Fig. 2

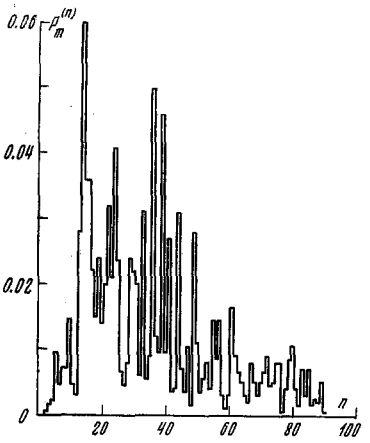

Fig. 3

sented in [1]. Here the quantity p_m means the magnetic field pressure averaged over the computational space interval, i.e., the dimensionless variables

$$p_m = \langle H_x^2 + H_y^2 \rangle = \frac{1}{J} \sum_{j=1}^{J} (H_{xj}^2 + H_{yj}^2)$$

Here J is the total number of grid nodes.

The calculations made for different parameters of the initial plasma state gave qualitatively the same picture: For comparatively small times ($0 < t \leq 20-30\gamma^{-1}$) there are nonlinear regular oscillations of the plasma and field characteristics, in which the average magnetic pressure p_m initially increases to large values which agree well with the analytic solution and then p_m "returns" practically to zero and the process repeats. In the course of time the numerical solution takes on quite different features: The regular oscillations of the magnetic pressure disappear and the average magnetic pressure p_m approaches some quasistationary level (see Fig. 1 in [1]). In this process the spatial distribution of the magnetic field and, naturally, the other system characteristics become stochastic. As was noted in [1], such changes in the nature of the solution for times $t \geq 30-50\gamma^{-1}$ are the consequence of the growth of uncontrolled "computing noise" in accordance with the plasma instability described by (2.1).

Thus, after the regular "laminar" oscillations under the influence of random perturbations the system transitions into the turbulent regime, in which the average magnetic pressure takes some quasistationary value. As was noted in [1], the magnitude of the mean-square turbulent magnetic field $\langle H_\perp^2 \rangle = p_m$ increases with increase of the degree of plasma anisotropy, reaching, for example, the value $\langle H_\perp^2 \rangle = 4$ for $p_\parallel^\circ / p_\perp^\circ = 50$ (see Fig. 3 in [1]), i.e., the average magnetic field $\sqrt{\langle H_\perp^2 \rangle}$ in the quasistationary state for such anisotropy becomes twice as large as the unperturbed field H_0.

Of considerable interest is the question of the stochastic turbulent oscillation spectrum in the quasistationary regime. We studied the dependence of the magnetic field energy density on the wavelength (or the harmonic number). The magnetic field energy density $p_m^{(n)}$ associated with the n-th harmonic was found from the equation

$$p_m^{(n)} = \frac{2}{(J-1)^2} (a_n^2 + b_n^2 + c_n^2 + d_n^2)$$

where

$$a_n = \sum_{j=0}^{(J+1)/2} H_{xj} \cos \frac{2jn\pi}{J-1}, \quad b_n = \sum_{j=0}^{(J+1)/2} H_{xj} \sin \frac{2jn\pi}{J-1}$$

$$c_n = \sum_{j=0}^{(J+1)/2} H_{yj} \cos \frac{2jn\pi}{J-1}, \quad d_n = \sum_{j=0}^{(J+1)/2} H_{yj} \sin \frac{2jn\pi}{J-1}$$

The harmonic wavelength equals $\lambda_n = \varkappa R/n$.

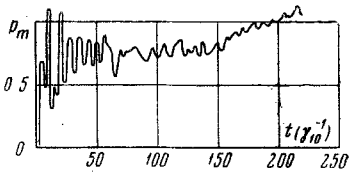

Fig. 4

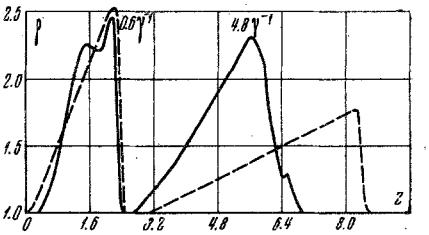

Fig. 5

The calculation results show that for comparatively short times after instability initiation all the magnetic energy is contained in the fundamental harmonic, which is specified as the initial perturbation. This would naturally be expected in the presence of regular oscillations. With transition into the turbulent region (when the oscillations become stochastic) the spectrum begins to change, since other harmonics begin to appear along with the fundamental. The harmonics with numbers n_0-1, $2n_0$, $2n_0-1$, where n_0 is the number of the fundamental, are excited first of all. However the higher harmonics $2n_0$, $2n_0-1$ decay quite rapidly (for example, in the case $p^\circ_\parallel = 30\,H_0^2/8\pi$, $p^\circ_\perp = 6.6\,H_0^2/8\pi$, $n_0 = 80$ this occurs for times of order $100\,\gamma_{80}^{-1}$). Most of the magnetic energy begins to transfer into the lower harmonics. The calculations show that the energy transfer process proceeds gradually – the harmonics whose wavelength is longer than that of the fundamental are excited later than those whose wavelength is shorter. Figure 3 shows the magnetic energy spectral density $p_m^{(n)}$ for quite long times ($t \approx 480\,\gamma_{80}^{-1}$, γ_{80} is the growth increment of the harmonic with $\lambda = \varkappa R/80$, obtained from linear theory) for the case $p^\circ_\parallel = 30H_0^2/8\pi$, $p^\circ_\perp = 6.6H_0^2/8\pi$. The increase of the energy associated with the lower harmonics is clearly seen in this figure. The magnitude of the energy of the individual harmonics is quite small: For example, in the subject case for $t \approx 480\,\gamma_{n0}^{-1}$ ($n_0 = 80$, $\lambda_{n0} = 80R$) the magnetic field energy density peak occurs at the harmonic with $n = 13$ ($\lambda_{13} \approx 490R$) and $p_m^{(13)} \approx 0.06H_0^2$.

Thus, the results of the numerical solution show that in the turbulent region in the presence of hose instability there is magnetic energy flux in the direction of small wavenumbers. It is possible that this is associated with the fact that the large wavenumber region does not "absorb" energy as in the case of hydrodynamic turbulence, since in the present case of Alfven turbulence the viscosity is nondissipative.

We also made a series of calculations in which the initial perturbation was taken in the form of the superposition of two or three circularly polarized waves with different lengths [in (2.2) $\mu = 2$ or 3, $f_i = f1_i = 0$]. The nature of the solution in the initial stage (meaning, of course, the stage which is already nonlinear but for comparatively small times $\sim 10-20\gamma^{-1}$) differs significantly from the case of a single circularly polarized wave: There is no "return" of the magnetic pressure, since there is superpositioning of two waves with different amplitude growth rates and different periods. The magnetic field becomes stochastic quite rapidly and the average magnetic pressure approaches the quasistationary level, just as in the case of the single initial monochromatic wave. Figure 4 shows the average magnetic pressure $p_m = p_m(t)$ in the case of an initial perturbation in the form of two circularly polarized Alfven waves, where one wave is half as long as the other. The calculations show that the turbulent magnetic pressure in the quasistationary regime in the presence of two or three initial waves is practically equal to the magnetic pressure in the case of a single initial wave for the same degree of plasma anisotropy. Hence we can apparently conclude that the quasistationary turbulent magnetic field level is independent of the instability excitation conditions.

To study the influence of hose instability on the shock wave structure, we made a series of calculations with the initial conditions (2.2), (2.4), (2.5) for $\mu = 1$, $f = f1 = 0$, $A \neq 0$, which correspond to specification at the initial time of a Riemann sound wave (with $\chi = 3$) and a transverse perturbation in the form of a circularly polarized Alfven wave. Figure 5 shows the density distribution in the wave at different times obtained from the numerical solution. The following parameters were used for this calculation

$$p_\parallel^\circ = 10H_0^2/8\pi, \qquad p_\perp^\circ = 7.5H_0^2/8\pi, \qquad A = 1$$

(the initial plasma density at the peak is twice the unperturbed density). In this figure the time is expressed in terms of the increments γ, calculated from the parameters of the unperturbed plasma state of outside the compression pulse. The degree of plasma anisotropy in the compression region is naturally greater than outside this region, since the longitudinal pressure is proportional to ρ^3 while the transverse pressure is proportional to ρ. Therefore, within the limits of the compression region, where the plasma density is

greater than the unperturbed density, the instability develops faster, since the increment is proportional to the difference of the pressures (longitudinal and transverse).

For comparison Fig. 5 shows the density distribution in a sound wave which propagates through the plasma in the absence of transverse perturbations. As we would expect, the initially symmetrical density distribution becomes distorted and the slope of the leading front increases until a discontinuity (shock wave) forms. In the calculations the steepness is limited by the magnitude of the computational (approximational) viscosity and the steady-state width of the front amounts to three to four nodes of the difference grid.

The presence of transverse perturbations and the associated hose instability leads to change of the profile and parameters of the wave propagating along the magnetic field. We see from Fig. 5 that this wave lags behind the sound wave, which is associated with the reduction of the "effective" adiabatic exponent χ because of the presence of the transverse motions; the connection between the pressure and density is not specified in the form $p \sim \rho^{\chi}$, but is found from the equation

$$\frac{d}{dt}\left(p\frac{1+H_{\perp}^{2}}{\rho^{3}}\right)=0$$

The most important result of the calculations is that the development of hose instability leads to reduction of the wavefront slope. This can be interpreted as the appearance of a viscosity associated with fluctuations of the plasma and field parameters in the presence of the instability resulting from the pressure anisotropy.

Thus, the numerical solution of the problem in a broad region of the parameters in the case of a single initial circularly polarized Alfven wave shows the following:

1) There are regular nonlinear oscillations for times of order $10-20\gamma^{-1}$ which agree well with the analytic solution;
2) at longer times the magnetic field becomes stochastic and transition to the quasistationary regime takes place;
3) the quasistationary level of the average turbulent magnetic field increases with increase of plasma anisotropy;
4) in the course of time as the turbulence develops the magnetic field energy transfers from the fundamental harmonic, given by the initial perturbation, into the longwave portion of the spectrum.

The numerical solution of the problem with 2-3 initial circularly polarized Alfven waves which differ in wavelength and amplitude shows the absence of return of the magnetic pressure in the initial stage to small values and independence of the quasistationary level on the instability excitation conditions.

The numerical solution also showed smearing of the compression wave leading front (in the presence of an initial longitudinal perturbation in the form of a Riemann sound wave) as a result of the appearance of the turbulent viscosity associated with hose instability development.

In conclusion the author wishes to thank R. Z. Sagdeev for suggesting the problem, his continued interest, and discussion of the results, and would also like to than R. N. Makarov for assistance in the calculations.

LITERATURE CITED

1. Yu. A. Berezin and R. Z. Sagdeev, "One-dimensional nonlinear model of anisotropic plasma instability," Dokl. AN SSSR, 184, No. 3 (1969).